Classifying North Atlantic Tropical Cyclone Tracks by Mass Moments*

JENNIFER NAKAMURA

Lamont-Doherty Earth Observatory, Columbia University, Palisades, New York

UPMANU LALL

Department of Earth and Environmental Engineering, Columbia University, New York, New York

YOCHANAN KUSHNIR AND SUZANA J. CAMARGO

Lamont-Doherty Earth Observatory, Columbia University, Palisades, New York

(Manuscript received 4 September 2008, in final form 12 May 2009)

ABSTRACT

A new method for classifying tropical cyclones or similar features is introduced. The cyclone track is considered as an open spatial curve, with the wind speed or power information along the curve considered to be a mass attribute. The first and second moments of the resulting object are computed and then used to classify the historical tracks using standard clustering algorithms. Mass moments allow the whole track shape, length, and location to be incorporated into the clustering methodology. Tropical cyclones in the North Atlantic basin are clustered with *K*-means by mass moments, producing an optimum of six clusters with differing genesis locations, track shapes, intensities, life spans, landfalls, seasonal patterns, and trends. Even variables that are not directly clustered show distinct separation between clusters. A trend analysis confirms recent conclusions of increasing tropical cyclones in the basin over the past two decades. However, the trends vary across clusters.

1. Introduction

Tropical cyclones lead to major natural disasters in the regions of landfall with devastating storm surges, flooding, and high winds. Named storms (NS) include all tropical cyclones reaching a maximum sustained wind speed of at least 18 m s^{-1} (35 kt) (Neumann et al. 1993). Their impact along the Atlantic coast of North and Central America is often catastrophic to life, ecology, property, wetlands, and coastal estuaries [e.g., in 1995 total mainland U.S. tropical cyclone damage averaged on the order of $5 billion; see Pielke and Landsea (1998)]. The severity and frequency of NS is consequently of great interest for disaster planning and mitigation. Determining the spatial characteristics of tropical cyclone frequency and intensity is of considerable importance for any study of past, present, and future hurricane impact or model validation. Clustering provides a way to assess the congruence in spatial characteristics such as track shape, genesis location, intensity, life span, seasonality, and landfall. The causal factors associated with each cluster, as well as the ability of numerical simulation models to simulate the frequency of each cluster, conditional on specified boundary conditions, could then be assessed. Macrolevel statistics of the conditional dependence of each cluster on antecedent conditions could also be assessed.

To a first approximation, hurricanes move in the direction that the mean tropospheric winds (over the depth of the storm) steer them. In the northern Atlantic, the northeasterly trade winds move the storms westward from the African coast. The prevailing flow around the subtropical high curves them northward approaching the North American coast and eastward in the middle latitudes. Elsner and Kara (1999) call this track shape the parabolic sweep. The position and strength of the subtropical high, the extratropical circulation, and the

* Lamont-Doherty Earth Observatory Contribution Number 7295.

Corresponding author address: Jennifer Nakamura, Lamont-Doherty Earth Observatory, The Earth Institute at Columbia University, 61 Rte. 9W, Palisades, NY 10964.
E-mail: jennie@ldeo.columbia.edu

DOI: 10.1175/2009JCLI2828.1

© 2009 American Meteorological Society

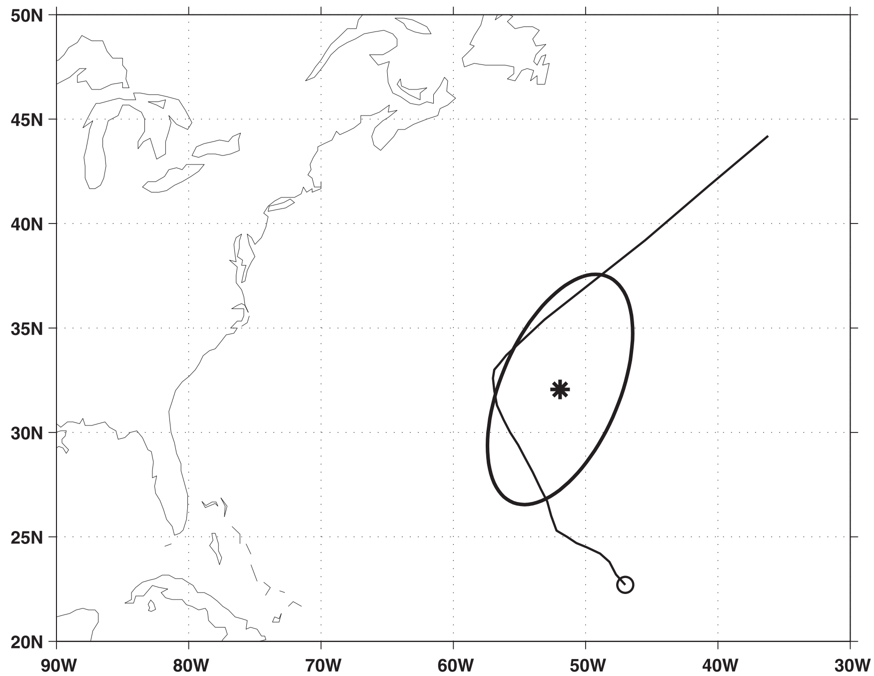

FIG. 1. Examples of the centroid (asterisk) and variance ellipse for the storm track. The track start is marked with a circle.

genesis location of the hurricane vary, allowing variation in track shape and length. Genesis location can be linked to the seasonality, sea surface temperature, wind shear, and position of the initial disturbance (Gray 1968, 1979; Henderson-Sellers et al. 1998). Both maximum wind speed (or intensity) and life span are linked to the genesis location and track shape as some locations/curvatures provide a longer time to intensify before encountering land or colder water. Landfall and the intensity of the storm at landfall are also associated with genesis location and track shape (Camargo et al. 2007).

Cluster analysis provides a way to objectively classify storms in a given ocean basin into subcategories depending on geographical properties of the storms (e.g., genesis, track location, and shape). Such classification can become useful for building predictive understanding on climate time scales. The K-means method (MacQueen 1967) is a common clustering method that has been used both with tropical (Elsner and Liu 2003; Elsner 2003) and extratropical cyclone tracks (Blender et al. 1997). The method is typically applied to vector data on select attributes and seeks to find k separations of the data such that the intercluster variation is maximized relative to the centroid of each cluster in the space formed by the vectors submitted. The application of this method to hurricane tracks (potentially specified as vectors defined by the x and y coordinates of the track) also faces the challenge that the tracks, and hence the data vectors with track coordinates, are of unequal lengths. The studies referenced above addressed this problem by using two points along the track (positions of maximum and final hurricane intensities), or dimensional vectors (centroids of the cyclone trajectories every 6 h for the first 3 days), respectively.

In the present study the entire track shape and length are taken into account by using the mass moments of the open curve that defines a full storm track. The first two moments are used and are defined and illustrated below. The first mass moment is simply the location of the x and y coordinates of the centroid of an object (in this case an open curve, and the centroid lies in the area interior to the curve, but not on the curve—see the asterisk in Fig. 1). The second moment is the variance (x, y, and xy directions). The second moment is illustrated by an ellipse in Fig. 1. Mathematically, the two moments are expressed as follows.

First moment:

$$\mathbf{M1} = \frac{1}{A}\int w(\mathbf{r})\mathbf{r}\,dx\,dy = \frac{1}{\sum_{i=1}^{n} w(r_i)}\sum_{i=1}^{n} w(\mathbf{r}_i)\mathbf{r}_i, \qquad (1)$$

where $\mathbf{r}$ is the coordinate vector (x, y) for a point on the track, $w(\mathbf{r})$ is a weight associated with that location (e.g., for the case of hurricane a measure of wind/storm intensity), the integral is taken over the open curve that defines the track, A is a normalization constant that reflects the total intensity over the track, and the sum on the right-hand side of the equation defines the discrete approximation to the integral over the track, using the n recorded locations of the track over the lifetime of the storm.

Second moment:

$$\mathbf{M2} = \frac{1}{A}\int w(\mathbf{r})(\mathbf{r} - \mathbf{M1})^2\,dx\,dy$$
$$= \frac{1}{\sum_{i=1}^{n} w(r_i)} \sum_{i=1}^{n} w(\mathbf{r}_i)(\mathbf{r}_i - \mathbf{M1}_i)^2, \qquad (2)$$

where $\mathbf{M1}$, $\mathbf{r}$, $w(\mathbf{r})$, A, and n are defined as in the first moment. In matrix format, the variance is the covariance matrix between the scalar components (x and y) of $\mathbf{r}$ giving three directions to the second moment of x, y, and xy.

These five numbers (two centroid and three covariance) then constitute the summary of the track information that is to be used to identify track clusters. The first moment establishes the location of the effective center of gravity of the storm track, while the second moment provides a measure of the shape of the storm. The classical covariance measure is usually explained as a measure of the orientation and length of the principal axes of an ellipse that describes the scatter of data in a plane. A similar interpretation applies here, with the qualification that the data of interest is not a scatterplot, but a section of a curve that is being approximated as an ellipse. Thus, if two tracks were perfect straight lines but with different lengths, then the second-moment matrix would identify the same orientation for both of them, but with a different spread along that direction. If the first track is a straight line and the other part of an ellipse, then from the covariance ellipse we would see that the length of the second principal axis is zero, indicating that there is no variation in that direction, while it would be nonzero for the curve, the magnitude increasing as the relative curvature increases. Further, if both tracks are curves, but one is convex and the other concave with respect to a particular reference frame, then the signs of the cross-covariance terms in the second-moment matrix are opposite, and one can recognize this condition. Thus, using the first two moments of a storm track one can get a measure of its central location, length, orientation, and also curvature. This allows one to get an approximation for most of the typical tracks that we observe. Complex features, such as tracks that curve back onto themselves or are concave in some sections and convex in others will require recourse to higher moments.

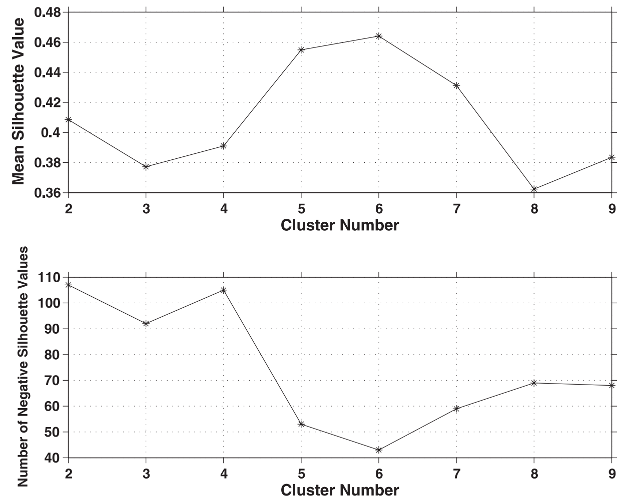

FIG. 2. (top) Mean silhouette values and (bottom) number of negative silhouette values.

The analysis of the track moments is performed here not during the evolution of a track but postmortem, taking into account the whole life cycle. Hence, this approach will not be useful for describing an evolving storm. Rather, it is intended for an analysis of historical data, especially for the identification of trends and associated causal factors for particular types of storms.

The dataset used is described in the next section along with some aspects of the clustering methodology. Section 3 presents associated results for northern Atlantic tropical storms, including a discussion of the attributes of the clusters in terms of spatial characteristics such as track shape, genesis location, intensity, life span, seasonality, and landfall. The last section compares our results with those from a selection of other methods.

2. Data

Atlantic basin historical hurricane track data (HURDAT), with information on storm position (latitude–longitude) every 6 hours available from the National Hurricane Center (NHC), was used. Only NS from 1948 to 2006 were retained for our analysis. Owing to routine aircraft reconnaissance missions into tropical cyclones beginning in 1944, details on the position of the hurricane structure are available. This has lead to greater accuracy in the 6-h position data.

Clustering methodology

A variety of methods for the identification of clusters from vector data are available. Here, we use the K-means method with a vector of five attributes per track: two for latitudinal and longitudinal centroids and three for the variance (latitudinal, longitudinal, and diagonal).

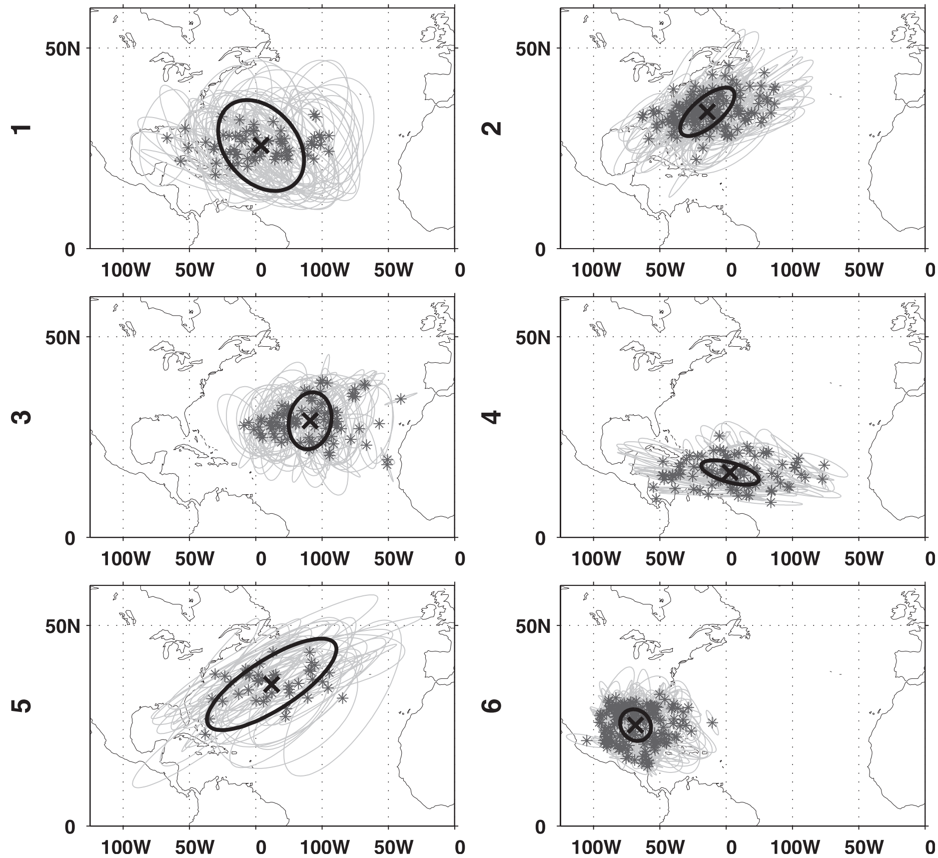

FIG. 3. Centroid locations (asterisks) and directional variance (light ellipses) for the six clusters. The mean centroid value is marked with a dark x, and the mean variance ellipse with a dark line.

The variance components contain much larger values than the centroid components. To give the centroid and variance equal weight in the cluster analysis, the variables are standardized (to mean zero and first standard deviation); each centroid column is multiplied by 0.5/2, and each variance column by 0.5/3 so that the centroid and the covariance are treated roughly on par as to their importance for clustering. Other weights that emphasize one or the other attribute could indeed be chosen.

Moments along the northern Atlantic cyclone tracks were estimated using wind velocity (or power) recorded along the track as a weight and also using uniform weights [$w(\mathbf{r})$ of ones in 1 and 2]. Each of the resulting data was then used in K-means cluster analysis. Results are presented for the uniform weight case. Separation between the clusters was distinct and clusters cohesive as tracks were grouped together in geographical regions. When wind velocity weights are used, tracks farther apart are added to the cluster.

The K-means clustering algorithm partitions the data into k clusters, with cluster centroids denoted by μ_i and coordinates as $x_{i,j}$, such that the variance across clusters defined below is maximized; J is the index over all points in cluster i ($i = 1 \ldots k$):

$$\text{var} = \sum_{i=1}^{k}\sum_{j=1}^{l}(x_{i,j} - \mu_i)^2. \tag{3}$$

The K-means cluster analysis package available in Matlab 7.3 considers multiple runs with random seeding of clusters. The optimal cluster number j is determined by the maximum mean and minimum number of negative

TABLE 1. Mean centroid and variance values for each cluster.

Cluster	Centroid x (°W)	Centroid y (°N)	Variance x	Variance y	Variance xy
1	58.38	25.69	168.25	128.29	−47.89
2	65.68	34.07	67.20	36.33	33.99
3	43.06	29.06	41.89	50.48	5.64
4	58.83	16.16	75.28	9.34	−14.98
5	55.20	55.20	381.27	129.95	171.38
6	87.32	25.15	21.74	15.57	−2.48

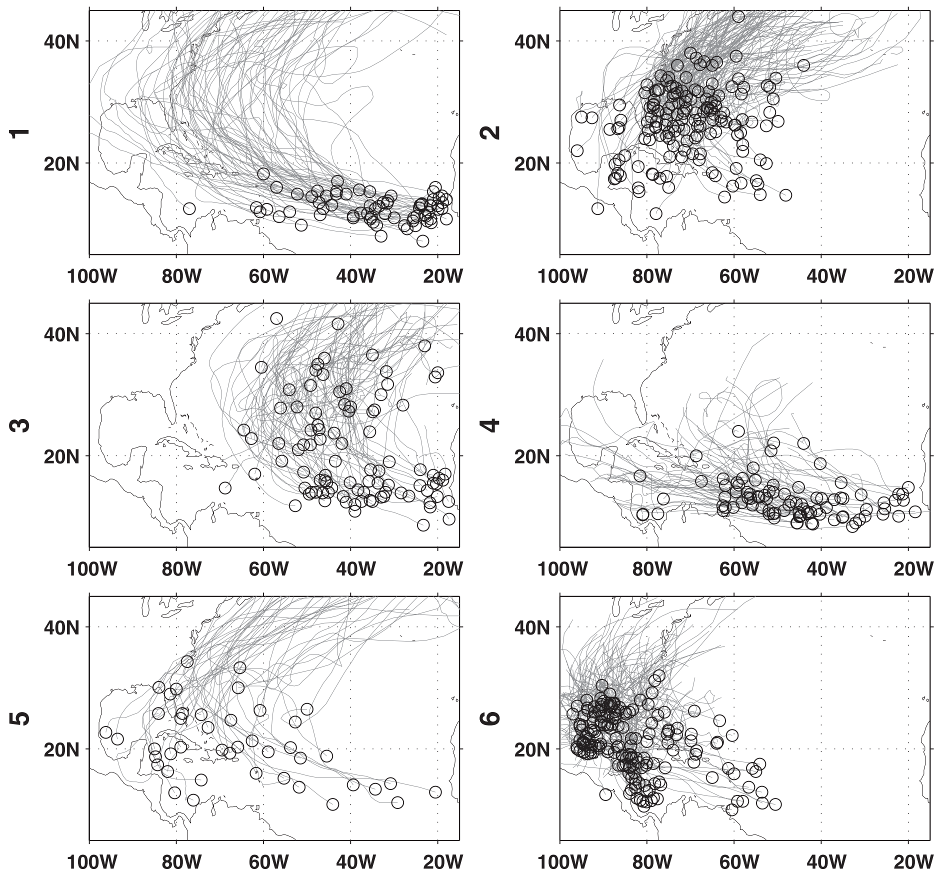

FIG. 4. Genesis location (circle) and the track (line) for the six clusters.

"silhouette" values. A silhouette is both a measure of how cohesive each cluster is and how well the clusters are separated. For i total points a silhouette (S_i) is defined as

$$S_i = \frac{\min(b_i) - a_i}{\max[a_i, \min(b_i)]}, \tag{4}$$

where a_i is the average distance from the ith point to the other points within the cluster and b_i is the average distance from the ith point to points in another cluster (Kaufman and Rousseeuw 1990). Silhouette values range from −1 to 1. Clusters with a high mean silhouette value are cohesive and negative silhouette values are possible misclassified points. Figure 2 shows the mean silhouette values (top) and number of negative silhouette values (bottom) for a selected run with the northern Atlantic hurricane data. Cluster numbers from two to nine run along the x axis. Note that the mean silhouette value for the six clusters is a maximum in the top panel of Fig. 2 and the number of negative silhouette values a minimum in the bottom panel, indicating the best choice of cluster number is six.

3. Cluster analysis results

a. Centroids and variance

The actual output of the K-means clustering is groups of centroid locations and directional variance (Fig. 3). Clear separation of the clusters can be seen in the groupings of the centroids and slope and size of the variance ellipses. The mean centroid value is marked with a dark x, and mean variance ellipse with a dark line. Table 1 presents the mean centroid location and directional variance for each cluster (1–6). Cluster 1 is centered

TABLE 2. Mean and range of tropical cyclone genesis locations for each cluster.

Cluster	Mean x genesis (°W)	Mean y genesis (°N)	Genesis x range (°W)	Genesis y range (°N)
1	34.60	12.61	77–18	7.2–18.2
2	70.50	26.64	96–44	11.7–44
3	39.35	20.76	68.8–17.4	8.6–42.5
4	46.83	12.76	81.6–14	8.4–24
5	65.89	20.67	96.2–20.5	10.9–34.3
6	83.16	20.77	97–50.5	10–32

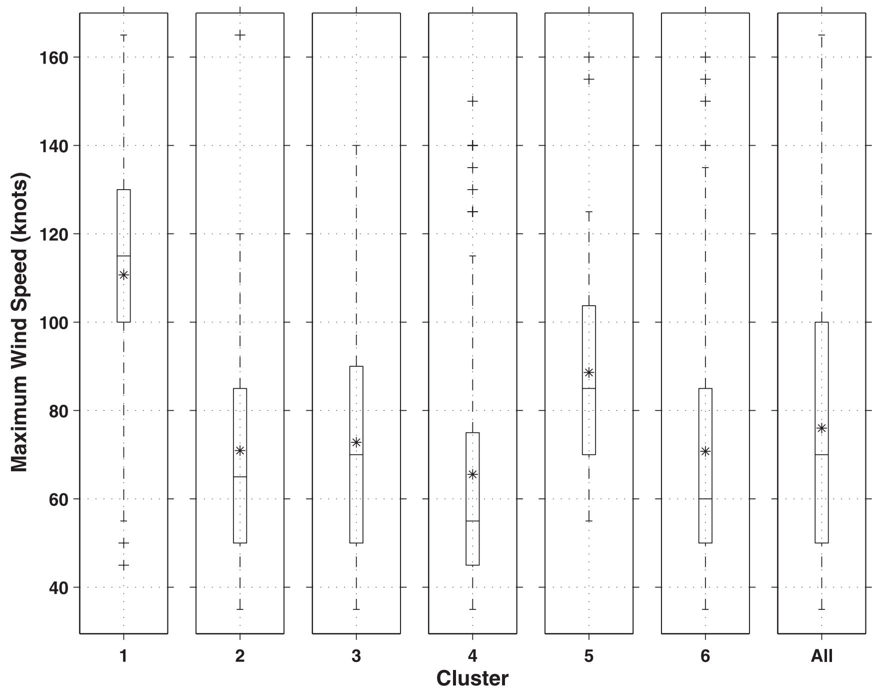

FIG. 5. The 25th and 75th percentiles (upper and lower bounds of the box), the mean (asterisk), the median (bar in middle), the bounds (dashed line), and outliers (plus signs) of the distribution of tropical cyclone maximum wind speed in each cluster and as a whole.

just west of midbasin with rounded variance ellipses (the mean variance x is approximately equal to mean variance y) and a slightly negative tilt (negative mean variance xy). The mean location of cluster 2 is slightly higher than that of cluster 1 near the eastern coast of the United States. The variance ellipses are elongated along the x axis with a positive tilt. Cluster 3 sits midbasin with rounded ellipses and nearly zero tilt. The farthest southern cluster is 4 and its ellipses are stretched along the x axis with a slightly negative tilt. The farthest north of all clusters is 5. It also has the largest ellipses, elongated along the x axis and heavily positively tilted. Cluster 6 is centered over the Gulf of Mexico and, like cluster 3, is rounded with near-zero tilt; it has the smallest variance ellipses.

b. *Genesis location and track shape*

Although the track location and shape are taken into account with the centroid and variance, the first reported location or genesis and actual track are not directly used in the entire analysis. Still, clear groupings can be seen in Fig. 4 with the genesis location as a circle and the track as a line. Table 2 presents the mean genesis location in each cluster along with the range of those first positions. Cluster 1 genesis locations fall roughly within the main development region of Goldenberg et al. (2001). These are Cape Verde hurricanes [Atlantic basin hurricanes that form close to the Cape Verde Islands (<1000 km) and become tropical cyclones before reaching the Caribbean] moving in a classic parabolic shape as described by Elsner and Kara (1999). They are the tropical cyclones forming farthest east of all the clusters and have the smallest genesis range in latitude. The tropical cyclones forming farthest north are in cluster 2. They have a diffuse genesis range in both latitude and longitude and move along the eastern coast of the United States. The largest genesis range in latitude is found in cluster 3 and these storms follow a flattened-shape parabola. The genesis location of cluster 4 resembles cluster 1 with a small genesis range in latitude in the Cape Verde region. What differentiates these tropical cyclones is the nearly straight track shape: they rarely venture above 25°N. The most diffuse in genesis location is cluster 5, with the largest genesis range in longitude. The tropical cyclones in cluster 5 are not full parabolas, but rather partial "hooks" or semiparabolas. Cluster 6 genesis locations are confined to the Gulf of Mexico and Caribbean, with the smallest genesis range in longitude. These tropical cyclones also tend to stay in the gulf.

c. *Intensity and life span*

The life span of a storm usually affects the size of the variance ellipse; that is, a longer track equals a larger ellipse unless the tropical cyclone is very slow moving.

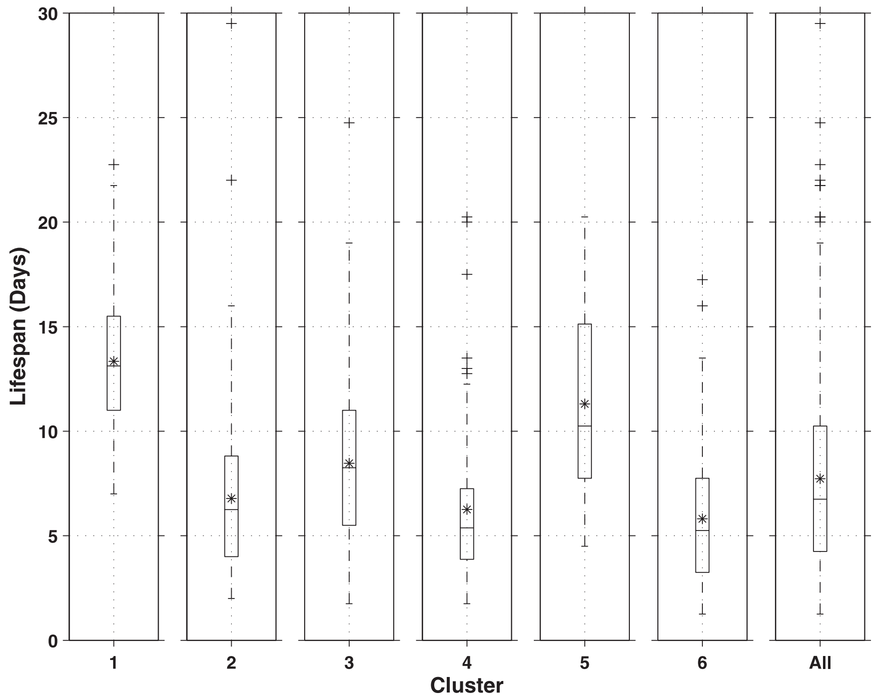

FIG. 6. As in Fig. 5, but for the life span (days) in each cluster and as a whole.

The next three figures, which explore the maximum wind speed (Fig. 5), life span (Fig. 6), and maximum intensity (Fig. 7), are box plots. These illustrate the 25th and 75th percentiles (upper and lower bounds of the box), the mean (asterisk), the median (bar in middle), the bounds (dashed line), and outliers (plus signs) of the distribution of tropical cyclones in each cluster and as a whole.

Maximum wind speed is categorized by the Saffir–Simpson scale as follows: tropical storm (TS), 35–64 kt; Category 1, 65–82 kt; Category 2, 83–95 kt; Category 3, 96–113 kt; Category 4, 114–135 kt; and Category 5, greater than 135 kt. Figure 5 shows the maximum wind speed in knots of the six clusters and all tropical cyclones. Table 3 presents the mean and median categories of the maximum wind speed. Cluster 1 is considerably stronger than the other clusters and the total, with cluster 5 coming in second. Clusters 2 and 3 are only slightly weaker than the total mean, keeping within the same category. Clusters 6 and 4 are weaker than the total with the median maximum wind speed falling in the TS category. The strongest, cluster 1, shows a negative skew distribution as compared to normal with the median in a higher category than the mean (majority of storms weaker than the mean) and the weakest, clusters 4 and 6, show a positive skew with the median in a lower category than the mean (majority of storms stronger than the mean).

Life span was converted from 6-h periods to days for easier viewing in Fig. 6. If ranked from longest to shortest, it follows the same pattern as the maximum wind speed except for the last two, which are nearly equal. The three longest clusters (1, 5, and 3) are longer than the total and the three shortest (2, 4, and 6) are shorter. The longer the life span, the longer the time the tropical cyclone has to intensify as long as the conditions stay favorable (i.e., warm waters and low shear). Life spans were all negatively skewed with the majority of the tropical cyclones lasting less time than the mean.

The power dissipation index (PDI) (Emanuel 2005) is a hybrid of the maximum wind speed and the life span and is used here as a measure of integrated intensity. Emanuel (2007) found the index to covary with low-level vorticity and vertical wind shear and correlate highly with sea surface temperature. PDI is defined as the simplified power dissipation index, as in Emanuel (2005):

$$\mathrm{PDI} \equiv \int_1^n V^3\,dt, \tag{5}$$

where n is the number of time steps with dt in seconds and V is the wind velocity in meters per second giving units of PDI in cubic meters per second squared. The large index values are multiplied by 1×10^{-11} for plotting ease. Not surprisingly, the combination of wind speed and life span shows cluster 1 to be the most intense, followed by cluster 5. These are the only two that are stronger than

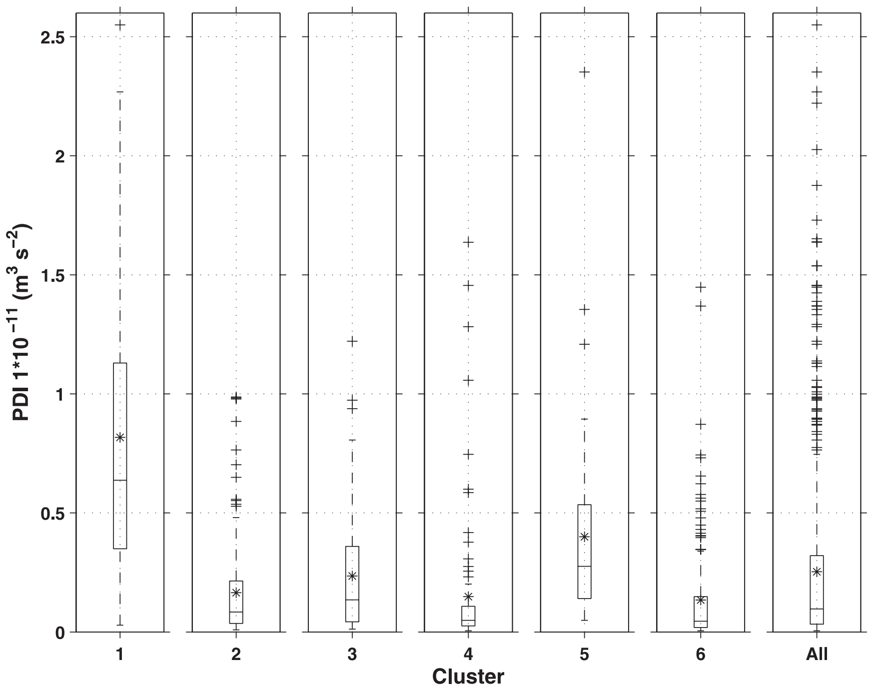

FIG. 7. As in Fig. 5, but for the tropical cyclone PDI multiplied by 1×10^{-11} in each cluster and as a whole.

the average of all. However, the distributions of clusters 2–6 show quite a few outliers, indicating that intense storms are possible in these clusters, but more of a rare event than for cluster 1. All the distributions are negatively skewed, just like the life spans, indicating that the majority of tropical cyclones are less intense than the mean.

d. Seasonality

If following the mariner's poem (Inwards 1898, p. 86),

June too soon.
July stand by.
August look out you must.
September remember.
October all over.

one would conclude that the North Atlantic hurricane season is four months long, from July through October. Indeed, looking at a box plot of storm month (Fig. 8) and not counting outliers, three of the clusters (1, 3, and 6) along with all storms show a four-month season from July to October. However, two clusters have a six-month season (4 and 5) from June through November and cluster 2 has an eight-month season from April through November. Outliers even show a tropical cyclone in February. Note that, due to the discrete nature of the month, sometimes the 25th or the 75th percentile and the median are the same, so for Fig. 8 the median is marked with a circle. The cluster means all fall in August (eight) and September (nine) with two medians in August (clusters 1 and 2), and the rest in September: September is to remember. Three clusters have a negative skew with more tropical cyclones occurring earlier than the mean (1, 2, and 3), and the other three along with the total having a positive skew with more occurring later than the mean.

e. Landfall

Landfall was inferred by applying a 1° land–sea mask and counting the number of storms that crossed from ocean to land between 5° and 45°N, 100° and 50°W. Table 4 presents the cluster number, number of tropical cyclones in each cluster, number of landfalls, and the

TABLE 3. Mean and median category of the maximum wind speed in each cluster and in all tropical cyclones.

Cluster	Mean	Median
1	3	4
2	1	1
3	1	1
4	1	TS
5	2	2
6	1	TS
All	1	1

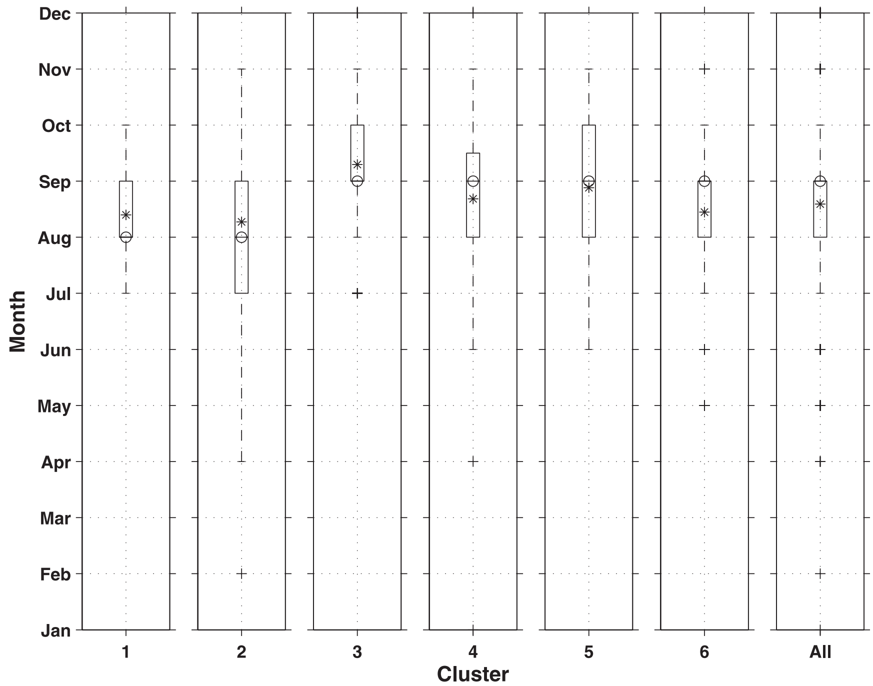

FIG. 8. As in Fig. 5, but for the tropical cyclone month in each cluster and as a whole.

percentage of landfall. Not only does cluster 6 have the highest number of storms, it also has the most landfalls. Tropical cyclones in that cluster do not have far to travel before they hit land. The most intense tropical cyclones in cluster 1 have a slightly higher percentage of hitting land than all storms; however, the number of storms in that cluster is fairly low. The second most intense storms in cluster 5 have the smallest number of tropical cyclones and a lower than all-storms landfall percentage. Clusters 2 and 4 both have a smaller landfall percentage than all storms; however, cluster 2 is well populated. Cluster 3 storms do not make landfall in the box chosen.

f. Trends

The Poisson distribution is ideally suited to model tropical cyclone counts as they are relatively rare occurring events. The probability of these rare events allowing counts per year (Y_i) with integer values of $y = 0, 1, 2, \ldots$, mean $\mu(x_i) > 0$, and the number of replications for each observation n_i is

$$P(Y_i = y) = \frac{[n_i \mu(x_i)]^y}{y!} e^{-n\mu(x_i)}. \tag{6}$$

For the Poisson distribution the mean is also equal to the variance. A simple generalized linear model for the mean (variance) that keeps counts positive is a log-linear model:

$$\theta = \log \mu(x_i). \tag{7}$$

The global log likelihood of parameter vector $\boldsymbol{\theta} = (\theta(x_i), \ldots, \theta(x_n))$ is

$$L(\theta) = \sum_{i=1}^{n} \log\{f[Y_i, \theta(x_i)]\}. \tag{8}$$

Within a smoothing window and taking advantage of this log link, the local log-likelihood function [product of probabilities given by Eq. (6)] is

$$L_x(\mathbf{a}) = \sum_{i=1}^{n} w_i(x) \mathbf{A}(x_i - x) Y_i, \tag{9}$$

where $\mathbf{A}$ is a vector of explanatory variables (fitting functions), $\mathbf{a}$ is a vector of the coefficients in a local

TABLE 4. Number of tropical cyclones (N) and landfalls and the landfall percentage for each cluster and for all tropical cyclones.

Cluster	N	Landfalls	Landfall percentage
1	70	32	46
2	157	35	22
3	94	0	0
4	92	26	28
5	43	14	33
6	174	148	85
All	630	255	40

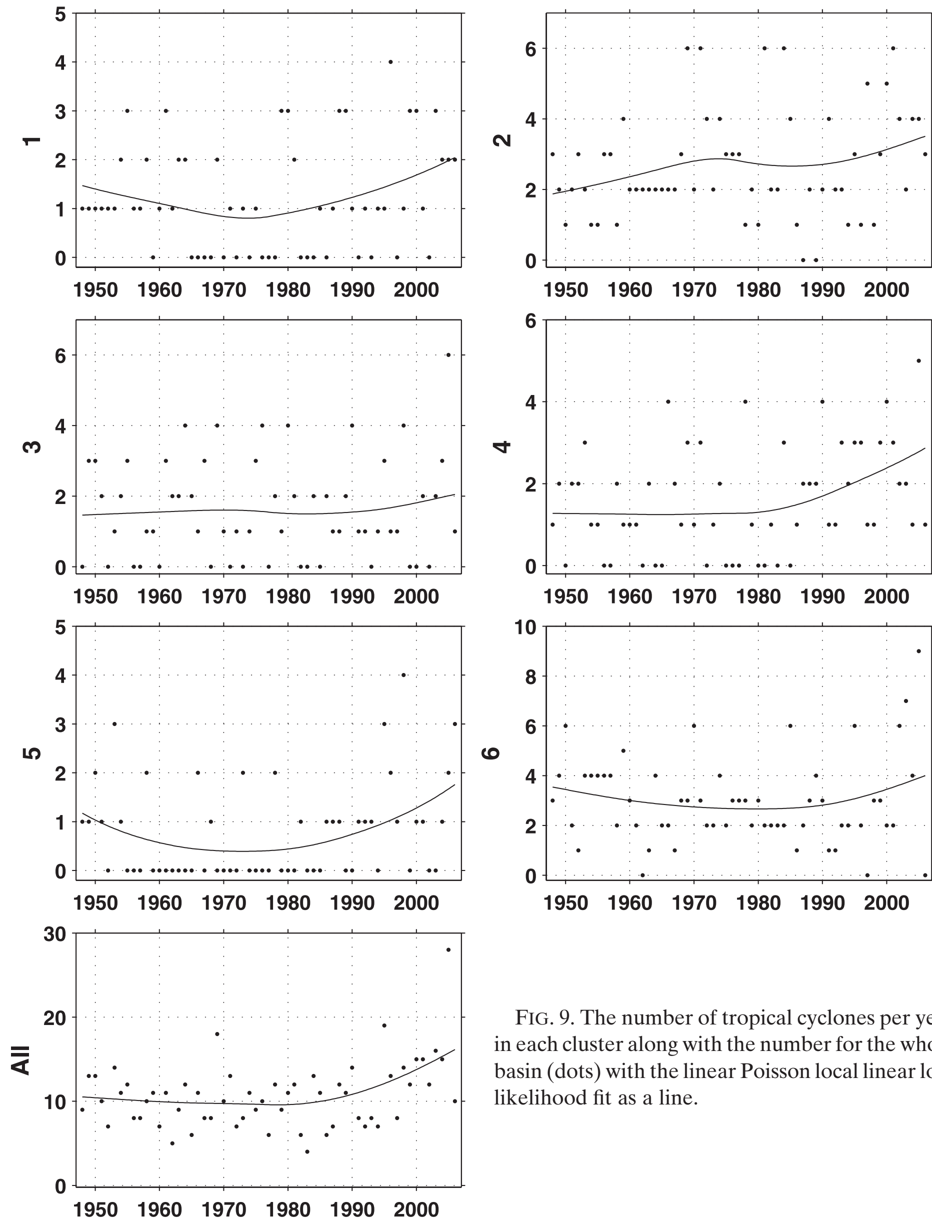

FIG. 9. The number of tropical cyclones per year in each cluster along with the number for the whole basin (dots) with the linear Poisson local linear log-likelihood fit as a line.

linear approximation ($a_0 + a_1x$), x_i are estimated points, x are the observed points, and w_i is the weight:

$$w_i(x) = W\left[\frac{x_i - x}{h(x)}\right], \quad W = (1 - |u|^3)^3, \quad |u| < 1, \tag{10}$$

where $h(x)$ is the bandwidth and W is the tricube weight function with smoothing parameter u.

The numbers of tropical cyclones per year in each cluster along with the number for the whole basin were analyzed by using this Poisson local linear log-likelihood (Fig. 9) by the Matlab version Locfit (Loader 1999). The fit is made in a moving window (nearest neighbor method) with 70% of the data (in this case 41 years) ensuring the local neighborhoods always contain a specified number of points (Loader 1999). The number of years runs along the x axis; the count on the y axis with the cluster name as the y label. All clusters show an upward trend in the last two decades, but some are more pronounced than others (clusters 1, 2, 4, and 5). Kossin et al. (2007) found that a trend for an increase in the NS counts in 1984–2004 in the North Atlantic basin was well supported. Goldenberg et al. (2001) also found recent upward trends in intense hurricanes.

The total PDI per year (multiplied by 1×10^{-11}) is plotted as dots with the Poisson local linear log-likelihood

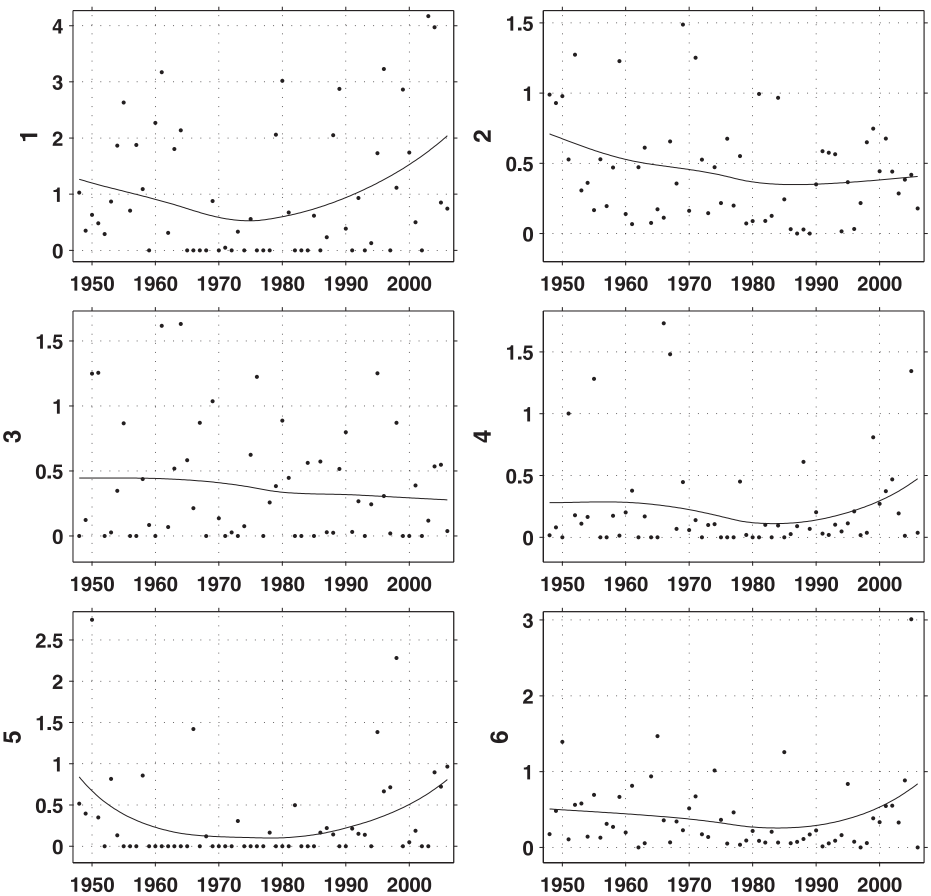

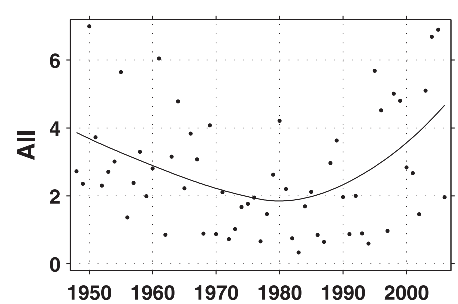

FIG. 10. PDI ($m^3 s^{-2}$) per year multiplied by 1×10^{-11} in each cluster along with the number for the whole basin (dots) with the linear Poisson local linear log-likelihood fit as a line.

as a line in Fig. 10. Year to year the index is highly variable. Emanuel (2007) found the variability to be linked to net surface radiation, thermodynamic efficiency, and average surface wind speed. It appears that the most intense clusters (1 and 5) have the strongest trend in the last two decades, although the last year (2006) showed a substantial downturn in cluster 1. Elsner et al. (2008) found an increased intensity of the strongest tropical cyclones due to an increase in ocean temperatures over the Atlantic Ocean and elsewhere. Both cluster 1 and the total were raised significantly by Hurricane Ivan in 2004. Ivan not only was a long track, but quickly intensified to Categories 4 and 5 and oscillated between the two. The all storms plot differs from Fig. 1 in Emanuel (2005) (Atlantic basin power dissipation index) because of the correction Emanuel applied to reduce the wind speed in the presatellite era and smoothing (Emanuel 2005, see the Supplementary Methods section). Landsea (2005) argues that the reduction is unwarranted because "in major hurricanes winds are substantially stronger at the ocean's surface than previously realized."

In summary, the trends for tropical cyclone counts and PDI vary by cluster. The evidence for linear trends over the period of record appears weak. However, there is evidence for an increasing trend in the last decade or so in both variables. The higher activity and intensity in the early part of the record is also notable for several of the

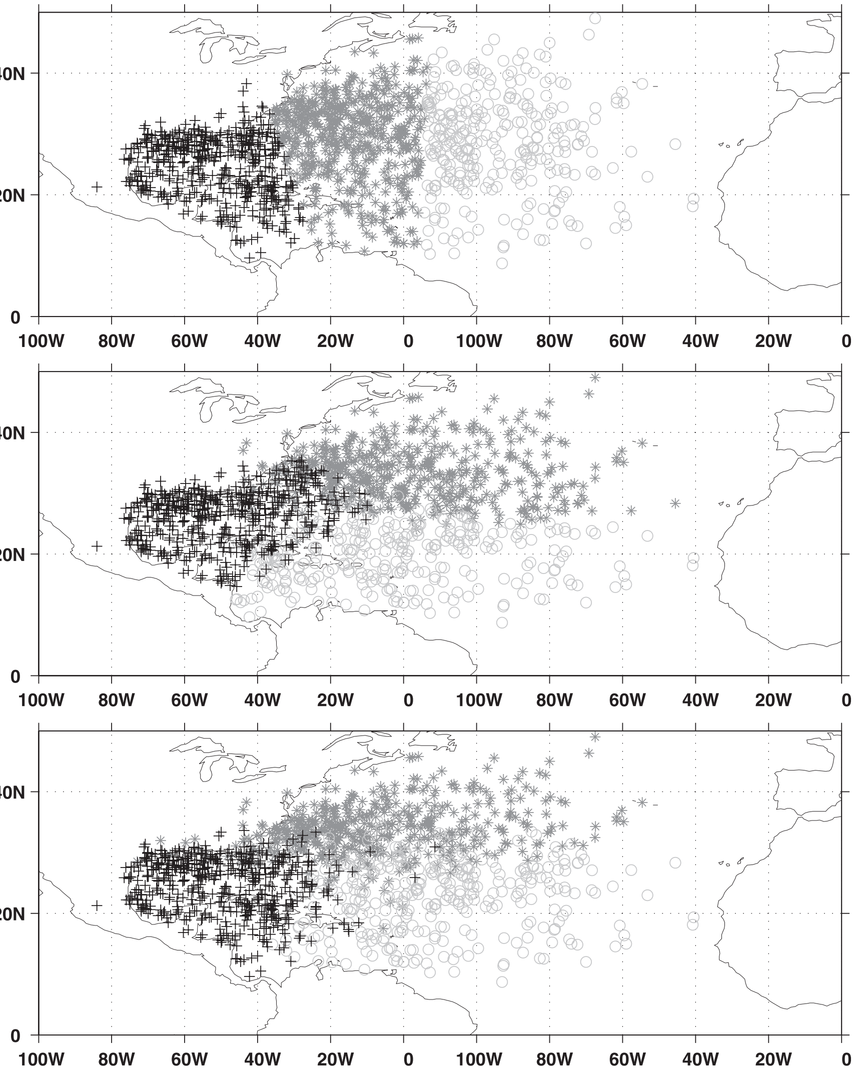

FIG. 11. Centroid locations of three clusters from 1851 to 2003 for (top) the *K*-means on centroids only, (middle) the *K*-means on the centroid and variance, and (bottom) the Camargo and Kossin (2008) regression mixture model.

clusters. The spatial shift in the PDI trends may be worthy of further investigation.

4. Discussion and conclusions

a. Contrasting other North Atlantic clustering studies

This is not the first study to use *K*-means clustering on North Atlantic tropical cyclones. Elsner (2003) clustered by latitude and longitude coordinates at maximum and final hurricane intensities and found three clusters. Elsner's study did not include TS tracks or portions of tracks resulting in shorter trajectories. Figure 1 of that paper shows the three clusters. Elsner finds the shorter trajectory, straight moving cluster (red) to be the most intense. By including the tropical storm part of the track, we found the longest tracks to be the most intense (correlation of 0.68 for length and intensity of all clusters, which is a significant *t* value for a two-tailed distribution at the 0.01 level). The three clusters are similar to the results that we found when only clustering centroids (Fig. 11, top); the cluster regimes have nearly north–south oriented breaks.

Camargo and Kossin (2008) have also completed preliminary clustering in the North Atlantic, incorporating the whole track length and actual location by using a regression mixture model on the entire HURDAT dataset. Three clusters were found: the Gulf of Mexico, Cape Verde, and eastern U.S.-born storms (11 bottom). When the *K*-means analysis is redone over a similar time period (1851–2003) for centroid and variance, the resulting clusters are strikingly similar (Fig. 11, middle). However, in this method, silhouette values indicate the optimal number of clusters to be six. In their North Pacific paper, Camargo et al. (2007) found a similar result of longer cyclone life spans leading to more intensification. The cluster number in these papers is based on an estimation of the diminishing return of log-likelihood plots and visual analysis. Camargo and Kossin (2008) also note that their finite mixture model produces better results than the *K*-means clustering because they take into account the whole track shape and location. Moments allow the use of the simple and computationally elegant *K*-means while also taking into account the whole track shape and location.

b. Summary

A novel approach for clustering storm tracks was developed using *K*-means clustering with the mass moments of centroid and variance. The centroid captures where the tropical cyclone is located and the variance describes the entire track shape. A summary of the results follows.

- A tropical storm track can be thought of as an open curve allowing computation of the first and second moments (centroid and variance, see Fig. 1).
- The *K*-means applied to the first two moments for each track provides a method for selection of clusters or groups. The group number is selected through the mean and number of negative silhouette values (Fig. 2).
- The resulting clusters (Fig. 3 and Table 1) have not only grouped centroid locations but also distinctly differently shaped variance ellipses.
- Although genesis locations of some clusters are diffuse (clusters 2, 3, and 5; see Table 2), the track shapes (Fig. 4) clearly follow a pattern: cluster 1 is the classic parabola, cluster 2 includes U.S. East Coast storms, cluster 3 the flattened parabolas, cluster 4 includes the straight-moving storms, cluster 5 the semiparabolas, and cluster 6 includes the Gulf storms.
- Both maximum wind speed and intensity were found to be linked to life span (correlations of 0.59 and 0.68, respectively, over all clusters: significant for a two-tailed distribution at the 0.01 level) with longer tracks producing higher maximum wind speeds and more intense tropical cyclones (Figs. 5–7).
- Half of the clusters showed the typical four-month-long Atlantic tropical storm season from July to October, while two clusters had a longer six-month season from June to November, and one cluster showed an eight-month season from April to November (Fig. 8).
- Landfall percentages of the clusters were clearly different, ranging from 0% to 85% (Table 4).
- Trends for the number of cyclones per year show an upward trend over the last two decades, but some are more pronounced than others (Fig. 9).
- Upward trends in maximum intensity of the most intense cyclone clusters were found to be stronger than those for all storms (Fig. 10).
- Results of the Elsner (2003) *K*-means study using two points along the track appear to correspond well to those obtained by only using the first moment of the tracks in the *K*-means (Fig. 11, top). Thus, Elsner's (2003) method uses only part of the information.
- Results of the Camargo and Kossin (2008) regression mixture model are similar to those obtained using both first and second moments in *K*-means (cf. Fig. 11 middle and bottom).

Future work will include exploring the meteorological conditions behind the six clusters. As tropical cyclone formation and movement is based on meteorological conditions, the hypotheses of clusters also being related is a sensible one. If clear connections are found, then known meteorological conditions can be linked to a particular class and shape of storms. Possible risk assessment applications include relating climate fields or indices to an increased or decreased chance of tropical cyclone genesis, genesis location, and track shape. These, in turn, can be related to landfall and possible landfall intensities, which is of interest to government planning boards and insurance companies.

Acknowledgments. We wish to thank the reviewers for constructive comments that improved the paper. This study was made possible by an Award from the Columbia University Office of Research Initiatives.

REFERENCES

Blender, R., K. Fraedrich, and F. Lunkeit, 1997: Identification of cyclone-track regimes in the North Atlantic. *Quart. J. Roy. Meteor. Soc.,* **123,** 727–741.

Camargo, S. J., and J. P. Kossin, 2008: Relationship of the Atlantic meridional mode with Atlantic hurricane tracks. Preprints, *28th Conf. on Hurricanes and Tropical Meteorology,* Orlando, FL, Amer. Meteor. Soc., P2A2. [Available online at http://ams.confex.com/ams/pdfpapers/137682.pdf.]

——, A. W. Robertson, S. J. Gaffney, P. Smyth, and M. Ghil, 2007: Cluster analysis of tropical cyclone tracks. Part I: General properties. *J. Climate,* **20,** 3635–3653.

Elsner, J. B., 2003: Tracking hurricanes. *Bull. Amer. Meteor. Soc.,* **84,** 353–356.

——, and A. B. Kara, 1999: *Hurricanes of the North Atlantic: Climate and Society*. Oxford University Press, 512 pp.

——, and K. B. Liu, 2003: Examining the ENSO-typhoon hypothesis. *Climate Res.,* **25,** 43–54.

——, J. P. Kossin, and T. H. Jagger, 2008: The increasing intensity of the strongest tropical cyclones. *Nature,* **455,** 92–95.

Emanuel, K. A., 2005: Increasing destructiveness of tropical cyclones over the past 30 years. *Nature,* **436,** 686–688.

——, 2007: Environmental factors affecting tropical cyclone power dissipation. *J. Climate,* **20,** 5497–5509.

Goldenberg, S. B., C. W. Landsea, A. M. Mestas-Nunez, and W. M. Gray, 2001: The recent increase in Atlantic hurricane activity: Causes and implications. *Science,* **293,** 474–479.

Gray, W. M., 1968: Global view of the origin of tropical disturbances and storms. *Mon. Wea. Rev.,* **96,** 669–697.

——, 1979: Hurricanes: Their formation, structure and likely role in the tropical circulation. *Meteorology over the Tropical Oceans,* D. B. Shaw, Ed., Royal Meteorological Society, 155–218.

Henderson-Sellers, A., and Coauthors, 1998: Tropical cyclones and global climate change: A post-IPCC assessment. *Bull. Amer. Meteor. Soc.,* **79,** 19–38.

Inwards, R., 1898: *Weather Lore*. Elliot Stock, 233 pp.

Kaufman, L., and P. J. Rousseeuw, 1990: *Finding Groups in Data: An Introduction to Cluster Analysis*. Wiley, 342 pp.

Kossin, J. P., K. R. Knapp, D. J. Vimont, R. J. Murnane, and B. A. Harper, 2007: A globally consistent reanalysis of hurricane variability and trends. *Geophys. Res. Lett.,* **34,** L04815, doi:10.1029/2006GL028836.

Landsea, C. W., 2005: Hurricanes and global warming. *Nature,* **438,** E11–E13, doi:10.1038/nature04477.

Loader, C., 1999: *Local Regression and Likelihood*. Springer, 309 pp.

MacQueen, J., 1967: Some methods for classification and analysis of multivariate observations. *Proc. Fifth Berkeley Symp. on Mathematical Statistics and Probability,* Berkeley, CA, University of California, 281–297.

Neumann, C. J., B. R. Jarvinen, C. J. McAdie, and J. D. Elms, 1993: *Tropical Cyclones of the North Atlantic Ocean 1871–1992*. National Climate Data Center–National Hurricane Center, 193 pp.

Pielke, R. A., Jr., and C. W. Landsea, 1998: Normalized Atlantic hurricane damage, 1925–95. *Wea. Forecasting,* **13,** 621–631.